Informatics in Medicine Unlocked 35 (2022) 101137

Contents lists available at ScienceDirect

Informatics in Medicine Unlocked

journal homepage: www.elsevier.com/locate/imu

Computer aided and experimental study of cinnamic acid analog for oxidative stress treatment: The therapeutic validations

Oluwafemi Adeleke Ojo [a,b,*], Akingbolabo Daniel Ogunlakin [a,b], Matthew Iyobhebhe [c], Christopher Busayo Olowosoke [d,e], Odunayo Anthonia Taiwo [f], Akolade Akinola [a,b], Daniel Fadiora [a,b], Adeshina Isaiah Odugbemi [b], Gideon Ampoma Gyebi [g], Charles Obiora Nwonuma [c], Adebola Busola Ojo [h], Omolara Olajumoke Ojo [h]

[a] Bowen University SDG 03 (Good Health and Wellbeing Research Cluster), Nigeria
[b] Phytomedicine, Molecular Toxicology, and Computational Biochemistry Research Laboratory (PMTCB-RL), Department of Biochemistry, Bowen University, Iwo, 232101, Nigeria
[c] Department of Biochemistry, Landmark University, Omu-Aran, Nigeria
[d] Department of Biotechnology, Federal University of Technology, Akure, PMB 704 Futa Road, Ondo, Nigeria
[e] Department of Biotechnology, Chrisland University, Abeokuta, Nigeria
[f] Department of Biochemistry, Chrisland University, Abeokuta, Nigeria
[g] Natural products and Structural (Bio-Chem)-Informatics Research Laboratory (NpsBC-RI), Department of Biochemistry, Bingham University, Karu, Nigeria
[h] Department of Biochemistry, Ekiti State University, Ado-Ekiti, Nigeria

A R T I C L E I N F O

Keywords:
Cinnamic acid analog
Oxidative stress
Hepatic toxicity
Purinergic
Molecular docking simulation
ADMET profiling
ex vivo studies

A B S T R A C T

Objectives: The purpose of this study was to investigate the therapeutic activity of the cinnamic acid derivative KAD-3 (ethyl 3-(4-methoxyphenyl) acrylate) on Fe^{2+}-induced oxidative hepatic damage via experimental and computer aided studies.
Methods: Oxidative hepatic damage was induced via incubation of tissue supernatant with 0.1 mM $FeSO_4$ for 30 min at 37 °C ex *vivo* with different concentration of KAD-3. Molecular docking, ADMET profiling, and density functional theory were conducted on the candidate to filter the properties of the drug candidate for drug design.
Key findings: GSH, CAT, and ENTPDase activities were reduced when hepatic damage was induced ($p < 0.05$). In contrast, a significant increase in MDA levels and an increase in ATPase activity were observed. When compared to control levels, KAD-3 treatment reduced these levels and activities ($p < 0.05$). KAD-3 demonstrated good bond formation (−5.8 kcal/mol, −5.6 kcal/mol), drug-likeness (no rule violation), and electronic properties (chemically reactive) as compared to the standard (quercetin). Molecular docking, ADMET profiling, and density functional theory predict the functional attributes of the drug candidate against ATPase and ENTPDase targets.
Conclusion: The findings from our study indicated that KAD-3 can protect against Fe^{2+}-induced hepatic damage by suppressing oxidative stress and purinergic activities.

1. Introduction

Oxidative stress has been gaining much interest recently because of its health implications. Oxidative stress is associated with a perpetual and continuous increase in the concentration of reactive oxygen species (ROS). This occurs when the antioxidant defense mechanisms are overridden by ROS's vast production [1]. Oxidative stress has been linked to different types of diseases, such as cancer, neurodegenerative diseases, high blood pressure, arteriosclerosis, and diabetes. According to reports, diabetes has been involved in over 1.6 million deaths worldwide as of 2019 [2]. Diabetes is known to exist in two different forms known as type-1, type-2, and gestational diabetes, with type-2 being the most commonly suffered among individuals across the world. Type-1 diabetes is associated with an insulin deficiency in the body of the individual suffering from the disease, which arises from the inability of the islet of Langerhans located in the pancreas to produce the

* Corresponding author. Phytomedicine, Molecular Toxicology, and Computational Biochemistry Research Laboratory (PMTCB-RL), Department of Biochemistry, Bowen University, Iwo, 232101, Nigeria.
E-mail addresses: oluwafemiadeleke08@gmail.com (O.A. Ojo), odunayotaiwo25@gmail.com (O.A. Taiwo).

https://doi.org/10.1016/j.imu.2022.101137
Received 14 November 2022; Received in revised form 21 November 2022; Accepted 23 November 2022
Available online 26 November 2022

hormone insulin, which is supposed to combat hyperglycemia in the body. Type-2 diabetes is associated with insulin resistance, which means insulin is produced but not utilized for different reasons like a sedentary lifestyle, obesity, being overweight, and the like. Gestational diabetes is when hyperglycemia occurs during the state of pregnancy [3]. Research has not been halted in seeking possible ways of managing this disease and the effects it brings with it. In light of these various developments, which have included several drugs and injection products and are now being exploited, the use of plants that have been reported to contain vital medicinal features that, when applied to manage diseases, show extremely promising results [4]. Also, researchers, food manufacturers, and scientists have shown tremendous interest in dietary polyphenols because they have demonstrated incredibly promising results when applied to diseases arising from oxidative stress, among others [5,6]. These polyphenols have also been reported to be abundant in nature as well as having a low-cost production rate, plus they have reported fewer side effects compared to the currently produced drugs [7]. Intervention catalysts are also known to be potent alternatives in drug discovery and the management of oxidative stress diseases. The catalyst used in this study is a cinnamic acid analog, which has been reported to be a generally safe reagent and has thus been applied in the food industry as an additive. Chinese cinnamon is a crystalline white phenolic compound that has a 50% sweet taste. A natural aromatic carboxylic acid with an acrylic acid group that is replaced at the phenyl ring, giving the acid either a trans or a cis configuration, is found in various plants, such as fruits, vegetables, grains, and even honey. Scientific studies carried out on this compound have stated that its derivatives are capable of producing beneficial effects such as anti-fungal [8], anti-inflammatory [9], anti-cancer [10], anti-malarial, hepatoprotective, and anti-tyrosinase potential [11]. Continuous research has been ongoing, and it is of great importance to evaluate the therapeutic validity of a cinnamic acid analog regarding the management of oxidative stress using experimental and computational validation.

2. Materials and methods

2.1. Chemicals

KAD-3 (ethyl 3-(4-methoxyphenyl) acrylate) and quercetin were products of SantaCruz Biotechnology, Heidelberg, Germany. All other chemicals were of analytical grade.

2.2. Ex-vivo studies

2.2.1. Experimental rats and organ preparation

Healthy male Wistar rats, weighing 250–300 g each, were purchased from the Department of Anatomy, Bowen University, Iwo, Nigeria. The rats were euthanized with halothane after being fasted for the previous night, and their livers were then removed, homogenized in 1% Triton X-100 in 50 mM phosphate buffer. Centrifuging the homogenate was done at 15,000 rpm and 40 °C. For *ex-vivo* research, the supernatants were collected in simple plain tubes. Rats were kept in agreement with the approved policies of BUI Institutional Animal Ethics Committee, and the study was given their approval (approval number: BUI/BCH/2022/0002).

2.2.2. Induction of hepatic injury ex-vivo

With a few minor modifications, the methods illustrated by Ref. [12] were used to induce liver injury *ex vivo*. In brief, 200 μL of the organ supernatant comprising various concentrations (30–240 μg/mL) of KAD-3 were combined with 100 μL of 0.1 mM $FeSO_4$. After incubation for 30 min at 37 °C, the samples were then used for biochemical analyses. The normal control used reaction mixtures with only the organ supernatant, and the negative control used reaction mixtures with only the tissue supernatant and $FeSO_4$.

2.3. Determination of antioxidant activities

2.3.1. Catalase (CAT) activity

CAT activity assay of KAD-3 was evaluated following the description of [12] with slight modifications. 780 μL of 50 mM phosphate buffer was added to 20 μL of tissue samples containing varying concentrations of the beet extract. Then, 300 μL of 2 M H_2O_2 was subsequently added and the absorbance was measured at 240 min for 3 min at a 1 min interval.

2.3.2. Reduced glutathione level

As described by Ref. [13], 600 μL of the tissue lysates were deproteinized by the addition of 600 μL of 10% trichloroacetic acid. The mixture was centrifuged at 3500 rpm for 10 min. 500 μL of the sample was transferred to a clean test tube and 100 μL of Ellman reagent was added to the mixture. This was allowed to incubate at 25 °C for 5 min, after which the absorbance was read at 415 nm. GSH was used as the standard.

2.3.3. Lipid peroxidation level

The lipid peroxidation inhibition capacity of KAD-3 was also assessed using the method described by Ref. [12]. Sequentially, 100 μL of 8.1% of SDS, 375 μL of 20% acetic acid, and 1000 μL of 0.25% thiobarbituric acid were added to 100 μL of the tissue lysates containing varying concentrations of the beet aqueous leaf extract. The reaction mixture was boiled for 60 min at 95 °C in a water bath. The mixture was allowed to cool at room temperature, and the absorbance was read at 532 nm.

2.4. Purinergic activity

2.4.1. Na/K^+ ATPase enzyme activity

Na/K^+ ATPase activity was determined using a slight variant of the method described by Ref. [14]. 1.3 mL of 0.1 M Tris-HCl buffer, 200 μL of 5 mM KCl, and 40 μL of 50 mM of ATP were added to 200 μL of the organ lysate comprising varying concentrations of KAD-3. The reaction mixture was incubated at 37 °C for 30 min using a mechanical shaker, after which 1 mL of distilled water and 1 mL of 1.25% ammonium molybdate were added to the mixture. The solution was then treated with 1 mL of 9% ascorbic acid and left to stay for 30 min. The absorbance was then read at 660 nm.

2.4.2. E-NTPDase enzyme activity

As described by Ref. [12], 40 μL of tissue lysates containing varying concentrations of KAD-3 were added to 400 μL of a reaction mixture containing: 1.5 mM CaCl2, 5 mM KCl, 0.1 mM EDTA, and 10 mM glucose. 225 mM sucrose and 45 mM Tris-HCl). The mixtures were then incubated at 37 °C for 10 min. Subsequently, 40 μL of 50 mM ATP was added and the mixture was further incubated at 37 °C in a mechanical shaker. To halt the reaction, 400 μL of 10% TCA was added to the mixture. The mixture was incubated on ice for 10 min, and the absorbance was measured at 600 nm.

2.5. Computational studies

2.5.1. Retrieval of protein three dimensional structure and determination of binding pocket

The alphafold model for ATPase (AF-P13637-F1) was used because of the inability to access the experimental PDB ID, while the X-ray crystallographic structure (6WG5) for ENTPDase was used for the docking analysis and best describe from Uniprot database at uniprot.org/uniprotkb?query as P13637 and Q9Y227 respectively. The experimental structure was then downloaded from the protein data bank www.pdb.org, and the unknown binding pocket predicted with FTsite server (https://ftsite.bu.edu) and protein plus server (https://proteins.plus/#dogsite) [15,16]. The generated PSE session file of the prediction was used to mark out the amino acids residues via PyMol software. Furthermore, PROCHECK server (https://servicesn.mbi.ucla.edu/

PROCHECK/) was employed to validate both structures by generation of a Ramachandran plot for the refined structure [17].

2.5.2. Retrieval of the synthesize and standard compound

The compounds KAD-3 (ethyl 3-(4-methoxyphenyl) acrylate) and Quercetin were retrieved using the ChemDraw software and PubChem database at https://pubchem.ncbi.nlm.nih.gov/, respectively.

2.5.3. Pharmacokinetics and ADME/toxicity profiling of ligands

The pharmacokinetic properties proffer the druglikeness, medicinal chemistry, lead likeness, toxicity and other physicochemical properties of a new drugs, phytochemicals, food additives and industrial chemicals candidates based on the absorption, distribution, metabolism, excretion, and toxicity behaviour [18]. This was carried out using the SwissADME (http://:www.swissadme.ch/index.php), admetLab prediction server (admetmesh.scbdd.com/service/evaluation) and admetSAR prediction tool webserver 8 (http://lmmd.ecust.edu.cn/admetsar2) [19].

2.5.4. Molecular docking simulation and 2D/3D interaction

The virtual structure-based docking simulation and complex interaction was carried out as reported by Ref. [20]. This method is use to show the best possible interaction pose between the small molecule and receptor for affinity generation. Prior to the analysis, the raw ligand files (KAD-3) was prepared using USCF chimera to add the polar hydrogen and charge. Using the python prescription software for the analysis, ATPase (Alphafold ID; AF-P13637-F1) Grid centre: x; 5.1462, y; −5.1996, z; −10.6907; Grid Dimension: 27.1597; y; 32.8993; z; 39. 1517. ENTPdase (PDB ID; 6WG5) Grid centre: x; 5.6189, y; 9.5081, z; 9.2914; Grid Dimension: 28.6533; y; 25.0000; z; 39. 27.4334 were generated for both protein active site initially determined using FTsite server. The proteins were selected as target in this computational study because of their significant expression correlation with the antioxidant signature. Also, known drug that have been reported in for the experimental screening of the associated antioxidant is quercetin, therefore was used as standard for study.

2.5.5. Density functional theory (DFT) calculation

The chemical reactivity of the compound was estimated using the Density Functional Theory calculation from the conformer distribution on Spartan software, utilizing B3LYP functional method and 6-31G* basis default setting for the geometry optimization [21]. The frontier molecular orbital (FMO) descriptor generated were as follow; highest occupied molecular orbital (HOMO) and lowest unoccupied molecular orbital (LUMO) energy. The HOMO and LUMO difference was used to determine the energy gap. Furthermore, the other quantum chemical descriptors which includes; hardness, softness, ionization potential, electronegativity, dipole moment, and electron affinity were determined using the formula as reported by Refs. [20,21].

2.6. Data analysis

Graphpad prism version 9.0.1 software was used to examine the data. The standard deviation of the mean (±SD) was used to represent the descriptive data. To compare the mean, a one-way ANOVA was conducted using Tukey's post hoc analysis with the significance level at $p < 0.05$.

3. Results

3.1. Antioxidant activity

Fig. 1 shows the reduced glutathione (GSH) level of the iron-induced liver toxicity, which displayed a significant ($p < 0.05$) increase in the GSH level following the treatment with KAD-3 in a dose-dependent manner when compared to the untreated group, whose level was greatly reduced. The catalase antioxidant level was also evaluated after

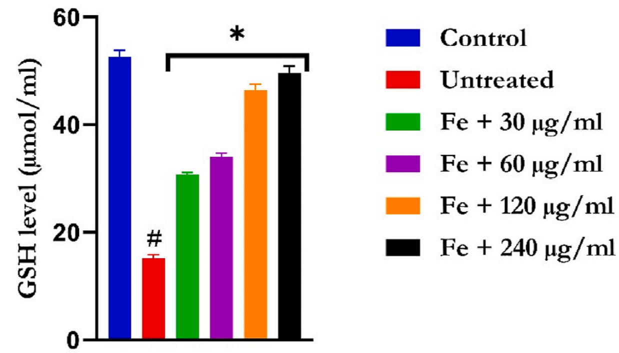

Fig. 1. Effect of Ethyl 3-(4-methoxyphenyl) acrylate on GSH level in iron-mediated oxidative hepatic toxicity.
Data = mean ± SD; n = 3. *Statistically significant compared to untreated tissue; #statistically significant compared to normal tissue.

the oxidative stress induction with iron, according to Fig. 2. The CAT level was seen to have also increased as the concentration of the KAD-3 treatment increased significantly ($p < 0.05$) when compared to the untreated group. For the MDA analysis shown in Fig. 3, the untreated group exhibited increased MDA activity when compared to the treated groups, which showed the ability of KAD-3 to reduce the activity of MDA significantly ($p < 0.05$).

3.2. Purinergic function

The ATPase activity is displayed in Fig. 4, following the induction of hepatic injury and treatment with KAD-3. From the displayed result, the treated groups showed a decrease in the ATPase activity in a dose-dependent manner when compared to the untreated groups, which displayed a higher level of concentration. Meanwhile, the ENTPDase activity (Fig. 5) indicated the reverse, showing that there was a significant ($p < 0.05$) increase in its activity in a concentration-dependent manner when treated with KAD-3 compared to the untreated, which had a rather low concentration.

3.3. Physicochemical, absorption, distribution, metabolism, excretion and toxicity

KAD-3 (Ethyl 3-(4-methoxyphenyl) acrylate) demonstrated good absorption and carbonate permeability with low bioavailability scores. The compounds exhibited a high volume of distribution (VD), high plasma protein binding (<92%), were non-inhibitors or substrates of glycoprotein, and were blood brain barrier permeant, which might be

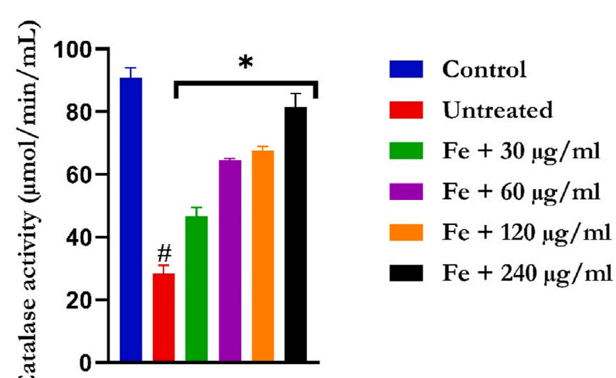

Fig. 2. Effect of Ethyl 3-(4-methoxyphenyl) acrylate on CAT activity in iron-mediated oxidative liver damage.
Data = mean ± SD; n = 3. *Statistically significant compared to untreated tissue; #statistically significant compared to normal tissue.

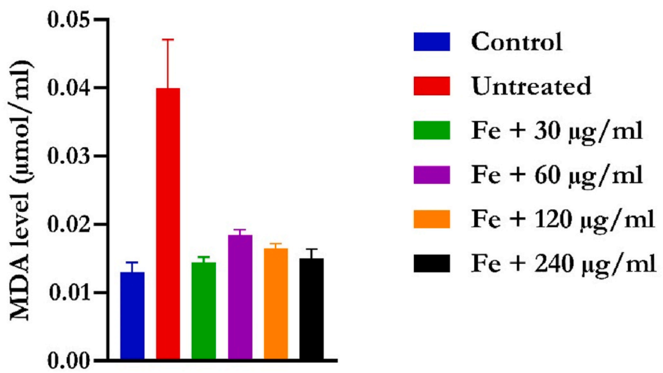

Fig. 3. Effect of Ethyl 3-(4-methoxyphenyl) acrylate on MDA level in iron-mediated oxidative liver damage.
Data = mean ± SD; n = 3. *Statistically significant compared to untreated tissue; #statistically significant compared to normal tissue.

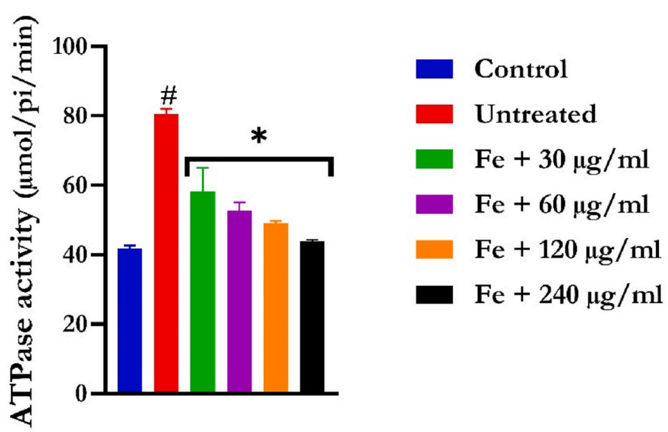

Fig. 4. Effect of Ethyl 3-(4-methoxyphenyl) acrylate on ATPase activity in iron-mediated oxidative liver injury
Data = mean ± SD; n = 3. *Statistically significant compared to untreated tissue; #statistically significant compared to normal tissue.

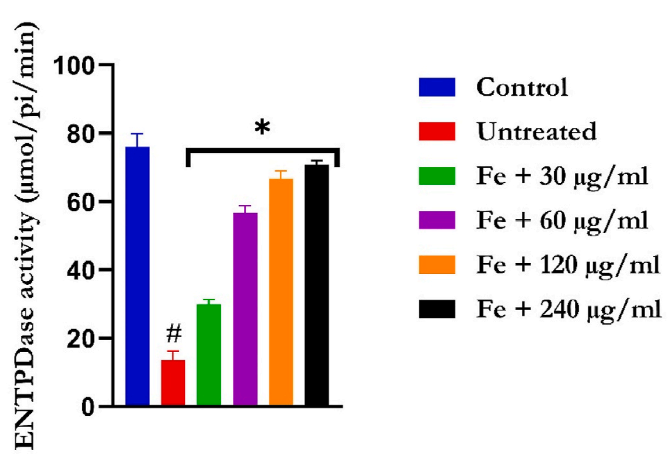

Fig. 5. Effect of Ethyl 3-(4-methoxyphenyl) acrylate on ENDTPase activity in iron-mediated oxidative liver injury
Data = mean ± SD; n = 3. *Statistically significant compared to untreated tissue; #statistically significant compared to normal tissue.

reconsidered for neurodegenerative disease studies (Table 1). The compound exhibits druglikeness potential, with neither of the Lipinski, Ghose, Veber, or Egan rules violated. However, the candidate's weak leadlikeness is shown by the violation of the XLOGP3>3.5 condition (Table 1).

Table 1
Adme/Tox properties of cinnamic derivative.

Compounds/ADMET-Profile	Properties	KAD-3 (Ethyl 3-(4-methoxyphenyl) acrylate)
Physicochemical	Formula	C12H14O3
	Molecular Weight (g/mol)	206.24
	Number of H-bond Acceptors	3
	Number of H-bond Donors	0
	Number of Rotatable Bond	5
	TPSA ($Å^2$)	35.53
	AlogP	2.27
	Water Solubility (LogS)	- 3.099
Absorption	XLOGP3	3.15
	WLOGP	2.16
	SILICOS-IT	2.63
	Human Intestinal Absorption	+ 0.9949
	$Caco_2$	+ 0.9430
	Human Oral Bioavailability	- 0.6714
	P-glycoprotein inhibitor	- 0.9821
	P-glycoprotein substrate	- 0.9861
Distribution	Volume Distribution (L/Kg)	0.822
	Plasma protein binding (100%)	76.7
	Blood Brain Barrier	+ 0.9744
Metabolism	OATP2B1 inhibitor	- 1.0000
	OATP1B1 inhibitor	+ 0.9490
	OATP1B3 inhibitor	+ 0.9725
	MATE1 inhibitor	- 0.8800
	OCT2 inhibitor	- 1.0000
	BSEP inhibitor	- 0.4734
	CYP3A4 substrate	- 0.5687
	CYP2C9 substrate	- 0.7982
	CYP2D6 substrate	- 0.8644
	CYP3A4 inhibition	- 0.9282
	CYP2C9 inhibition	- 0.9355
	CYP2C19 inhibition	- 0.8036
	CYP2D6 inhibition	- 0.9509
	CYP1A2 inhibition	+ 0.8150
Excretion	Clearance (mL/min/kg)	10.026
	Half life	0.445
Toxicity	Carcinogenicity (binary)	- 0.7303
	Hepatotoxicity	- 0.6500
	Respiratory toxicity	- 0.9333
	Reproductive toxicity	- 0.6556
	Mitochondrial toxicity	- 0.9500
	Nephrotoxicity	- 0.6531
	Acute Oral Toxicity (c)	III 0.8565
	Ames Mutagenesis	- 0.7800
Druglikeness	Lipinski Violation	Nil
	Ghose Violation	Nil
	Veber Violation	Nil
	Egan Violation	Nil
Medicinal Chemistry	PAIN Violation	0
	BRENK Violation	1
	Leadlikeness	No (MW < 250)

3.4. Structure validation and molecular docking

Prior to docking, the structural validation using Ramachandran plot shows that both refined protein has over 90% of the amino acids residue in the favored regions. Molecular docking was conducted to further screen the compound under study for binding affinity to the proteins after proper preparation and removal of non-amino acids residues. The results of the docking show conventional and carbon hydrogen interaction between the ligand and ATPase (Fig. 7) while akyl interaction was revealed for the ENTPDase (Fig. 8). Although the binding affinity were limitedly suitable compared to the standard (Quercetin), but can be improved (Table 2).

3.5. Density functional theory

Table 3 shows Gibb's free energy, dipole moment, enthalpy, and electronic energy calculated for the studied compounds. Quercetin has higher free energy, enthalpy, and energy of −1103.98758 au, −1103.92934 au, and −1104.17645 au than KAB-3, which has −691.161729 au, −691.109939 au, and −1104.17645 au, respectively.

Fig. 9 represents the HOMO/LUMO of the newly designed compound KAD-3 with a blue and red color sphere, which indicates the positive and negative regions of the molecular orbital.

From the data below in Table 4, the global reactivity descriptor calculations (ionization potential (I), electron affinity (A), chemical hardness (η), chemical softness (ζ), electronegativity (χ), chemical potential (μ)) further rely on the HOMO/LUMO energy for an in-depth chemical stability and reactivity study of the compound.

4. Discussion

According to Ref. [12], iron promotes the generation of reactive oxygen species (ROS), which leads to the onset of lipid peroxidation. The Fenton reaction produces a highly reactive hydroxyl radical when iron II (Fe^{2+}) interacts with H_2O_2, which could interfere negatively with the various metabolic processes involving proteins, lipids, and nucleic acids. The KAD-3 Fe^{2+} chelating activity could yet prove useful in the management of oxidative stress.

Hydrogen peroxide (H_2O_2) is not considered a radical because it possesses no unpaired electron, which makes it a little less reactive than ROS. When it is made to react with iron, then its impact is felt because it then becomes very reactive and causes major oxidative damage. The radical known as hydroxyl radical (•OH) is the most toxic and lethal form of the produced ROS. It is a very powerful oxidizing agent that can react very quickly with its surrounding chemicals without even selecting as fast as possible. This process operates by a process known as the Fenton reaction, in which iron (II) (Fe^{2+}) is oxidized by H_2O_2 into iron (III) (Fe^{3+}) to form a hydroxyl radical and hydroxide ion (OH^-), which causes injury and damage to the liver [22]. Following the induction of oxidative stress, decreased CAT and GSH activity was observed and could be linked to the fact that a pro-inflammatory action could be taking place in the liver as a result of the iron injury. Following the treatment with KAD-3, there was an increase in both GSH (Fig. 1) and CAT (Fig. 2) activities, which points out that there has been a regeneration of these antioxidants, which are now scavenging the free radicals. Thus, catalase has been known to be majorly involved in the cellular defense mechanism by suppressing all the buildup of H_2O_2 formed, indicating an antioxidative impact on ferric-induced oxidative hepatic damage. Also, the reduced glutathione (GSH), which is increased in the KAD-3 groups, in this case, indicates that the released ROS are being scavenged directly by the GSH enzyme, and it also serves as a cofactor for the enzyme glutathione peroxidase (GPx) in metabolizing hydrogen peroxide (H_2O_2) and lipid peroxides [23]. Previous studies on the use of antioxidants in the management of hepatic injury complications have recorded similar findings [3,24,25].

The result of the MDA (Fig. 3) signifies lipid peroxidation, which is a non-enzymatic antioxidant that plays a crucial role in combating the generated oxygen and hydrogen peroxide by dismutation of the produced oxygen radicals and damaging the peroxides that were produced as a result of oxidative stress. Increased MDA levels in the untreated group show the impact of liver injury damage as well as the presence of ROS in abundance, and this is in line with the findings of [3,26,27]. The reduced level of MDA observed indicates that KAD-3 shows great potential for influencing the dismutation of free radicals by the reduction of MDA.

The liver is responsible for major metabolic activities and thus requires energy to function properly. The level of ATPase activity (Fig. 4)

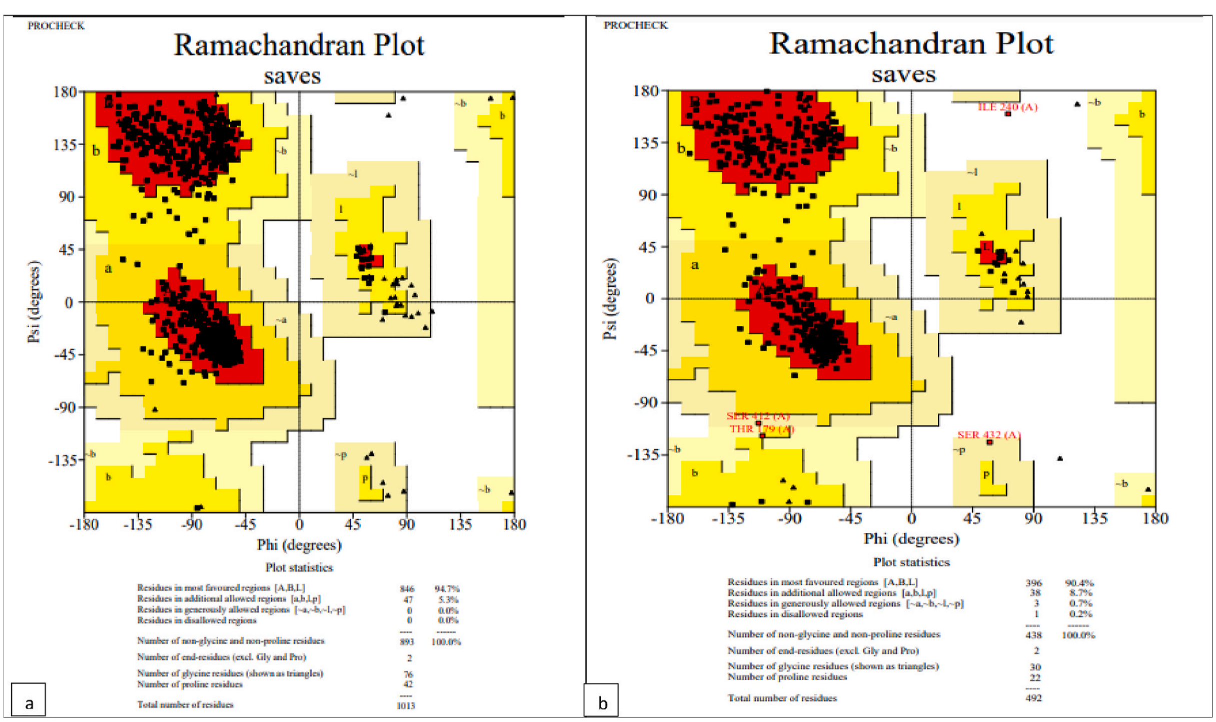

Fig. 6. Ramachandran plot validation the refined 3D structures. a; ATPase, b; ENTPDase.

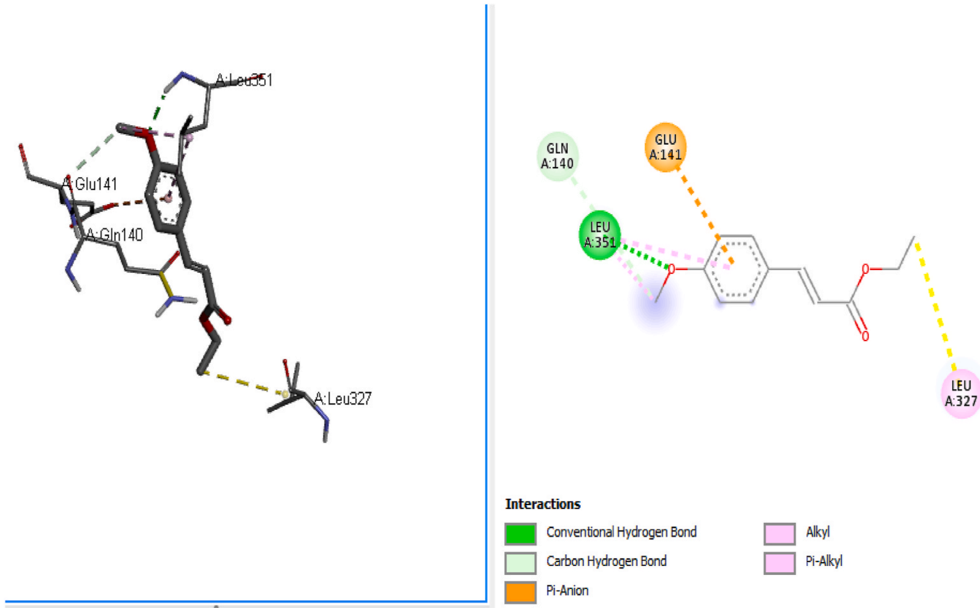

Fig. 7. 3D and 2D ATPASE-KAD 3 complex.

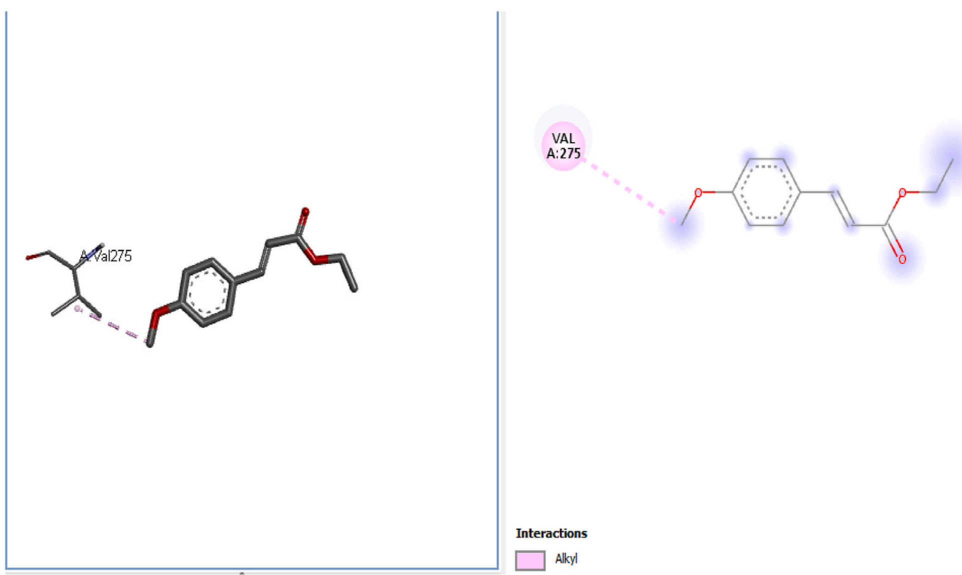

Fig. 8. 3D and 2D ENTPDASE-KAD3 complex.

Table 2
Docking score of the protein-ligand.

SN	COMPOUND/PROTEIN	BINDING AFFINITY (Kcal/mol)	
		ATPase	ENTPdase
1	KAD-3	−5.8	−5.6
2	QUERCETIN	−7.6	−7.1

observed shows an elevated level of the enzyme. This indicates liver damage when compared with the treated groups that tend to reduce in a dose-dependent manner, which suggests that KAD-3 is acting on the enzymes and effectively making use of them to release energy to combat the ROS in the cell. ENTDPase activity (Fig. 5) shows a decreased level in the untreated compared to the KAD-3 treated, which shows an increase in a dose-dependent manner, which could be a pointer to the fact that the injury inflicted upon the liver has been taken care of and that normal energy metabolism is taking place. These findings are similar to those of [28], where plant extracts exhibit the same properties.

Table 3
Molecular weight, electronic energy, enthalpy, Gibb's free energy values obtained via DFT at the B3LYP/6-31G* level.

Compounds/Parameters	Molecular weight (amu)	Dipole moment (Dyde)	Energy (au)	Gibb's free energy (au)	Enthalpy (au)
KAD-3	206.241	3.67	−691.362077	−691.161729	−691.109939
QUERCETIN	302.238	0.22	−1104.17645	−1103.98758	−1103.92934

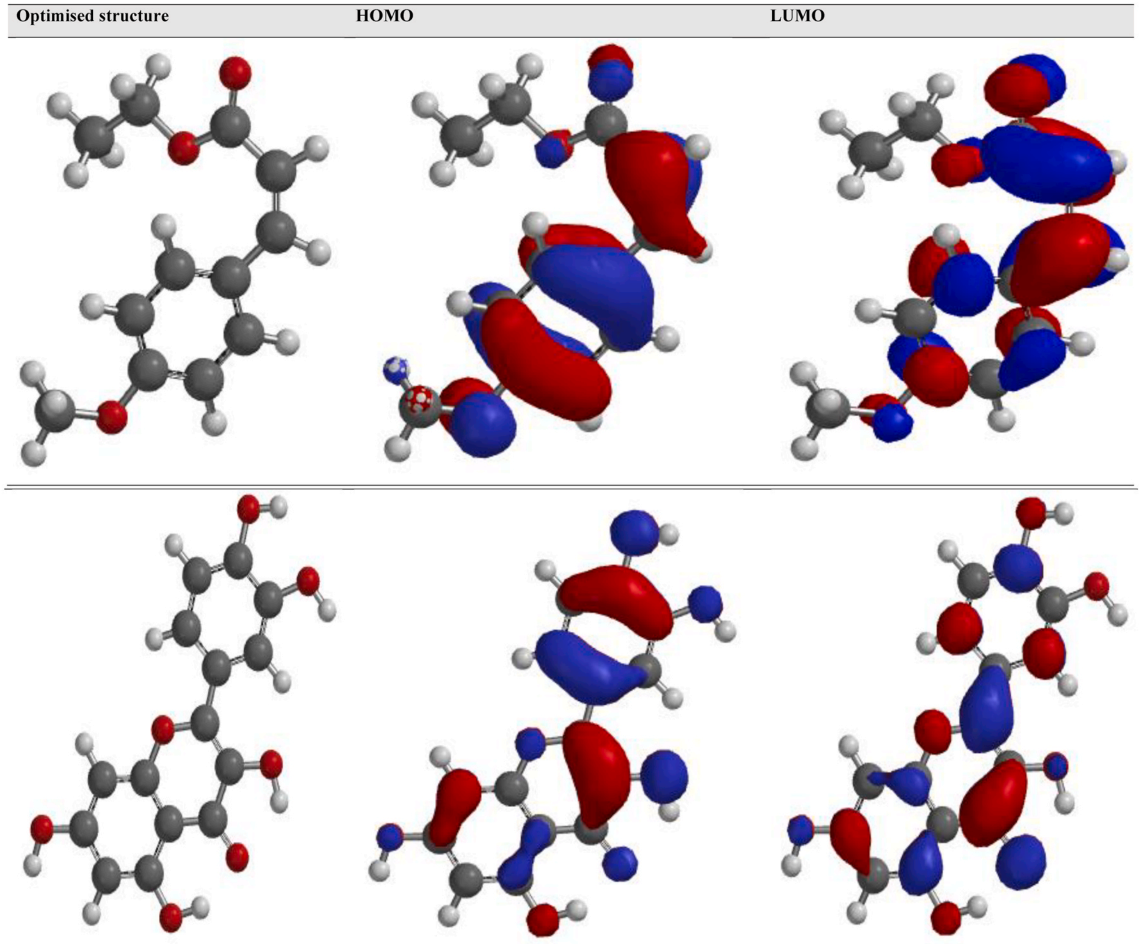

Fig. 9. The stabilized structure of KAD-3 and Quercetin compounds.

Table 4
Chemical reactivity parameters obtained via DFT at the B3LYP/6-31G* level.

SN	Compounds	E_{HOMO} (eV)	E_{LUMO} (eV)	E_g (eV)	I (eV)	A (eV)	η (eV)	δ (eV^{-1})	μ (eV)	χ (eV)
1	KAD-3	−5.82	−1.42	4.40	5.82	1.42	2.20	0.45	−3.62	3.62
	QUERCETIN	−5.48	−1.84	3.64	5.48	1.84	1.82	0.54	−3.66	3.66

Sodium potassium pump (Na+/K + ATPase) is a transmembrane protein complex studied for its ion pumping and osmotic balance functions, in addition to the scaffolding attribute in all higher eukaryotic cells [29]. Recently, findings on the association of cardiotonic steroids (CTS) mediated signal transduction through the Na/K-ATPase were identified to link with reactive oxygen species (ROS) generation, which are capable of initiating the signal cascade that demonstrated significance in oxidative stress related disease states such as obesity, atherosclerosis, heart failure, uremic cardiomyopathy, and hypertension [30]. While several reports have noted Na^{+}/K^{+} ATPase inhibition as a novel approach to limit the oxidative stress signaling pathway contributing to numerous diseases, this has significant therapeutic potential for the pathologies rooted in ROS [30–33]. Similarly, ecto-nucleoside triphosphate diphosphohydrolases (E-NTPDases) are a family of cell surface and lumen-associated enzymes in certain organelles that serve as major regulators of purinergic signaling, and some are possibly involved in protein synthesis [34,35]. Lately, findings have indicated the role of proteins in regulating crucial physiological processes such as immunity and cancer [35,36]. Hence, the inhibition was proposed for therapeutic intervention [34,37]. The mechanism for which this works is through the alteration of E-NTPDase activity, thus it encourages the availability of adenosine (protector of brain from neuronal dysfunction) in the synaptic cleft that may interrupt the release of other neurotransmitters. However, the associated overexpression of the ATPase with the inhibition of ENTPDase indicates the possibilities of signaling influx that can increase harmful ROS, Hence, this encourage for inhibition of both protein counterparts for a balanced activity [34].

The physicochemical and ADME/Tox properties act as precursors for the design and development of druggable compounds. In this study, we evaluated such properties on the synthesized quercetin derivative. The physicochemical properties of KAD-3 reveals the molecular weight (206.24 g/mol), rotatable bond (5), AlogP (2.27), Water solubility (-3.099), etc., as indicated in Table 1 to be much within acceptable range. More so, the ADME/Tox, druglikeness, medicinal chemistry of KAD-3 possesses data close to the recommended standard previously reported by [38].

Accordingly, a TPSA $<$ 79 Å2 and a WLogP less than 6 were reported to possess a BBB crossing potential (a microvascular unit that protects drug permeability to the brain), a property suitably important for CNS therapeutics [18,39], and to reduce toxin access to the brain. Also, the derivative stands as a promising non-substrate or inhibitor of the majority of the superfamily of Cytp450 essential for metabolism, except for

OATP1B1, OATP1B3, and CYP1A2 inhibition [16]. Additionally, the compound excretion properties are predicted to have a short half-life (0.445) and moderate clearance rate (10.026). The toxicity profile of the compound was appropriately negative for carcinogenicity (-0.7303), hepatotoxicity (-0.6500), reproductive toxicity (-0.6556), etc., and further classification in stage III (slightly toxic) of the acute oral toxicity potential. The derivative is a good drug choice due to its distinctive druglikeness potential and lack of violations of either of the four rules (Lipinski, Ghose, Veber, and Egan), but it is indicated as a poor lead-likeness due to its molecular weight violation (MW < 250).

The analysis of the Ramachandran plot generated using PROCHECK server showed that for refined ATPase structure, 94.7% of the amino acid residues was in the most favored regions, 5.3% were in the additional allowed regions, 0.0% were in the generously allowed regions, and 0.0% were in the disallowed regions (Fig. 6a). Whereas, for refined ENTPDase structure, 90.4% of the amino acid residues was in the most favored regions, 8.7% were in the additional allowed regions, 0.7% were in the generously allowed regions, and 0.7% were in the disallowed regions. This indicated the structural validation of the protein was relevant to proceed with the other downstream analysis (Fig. 6b).

A virtual molecular docking analysis was used to determine the potential of KAD-3 (ethyl 3-(4-methoxyphenyl) acrylate) to bind to the ATPase and ENTPDase targets. A conventional and carbon hydrogen bond interactions was observed between the compound (KAD-3) and the Leu 327, Leu 351, and Gln 140 amino acid residues of the protein. Additionally, other hydrophobic bonding interactions were identified as pi-anion, pi-akyl, and akyl bonds with Glu 141 and Leu 327, respectively (Fig. 7). However, there was limited visible bonding interaction between the compound and its ENTPDase counterpart, with just akyl bonding with Val 275 (Fig. 8). The characteristically low binding affinity displayed by the docked pose in comparison to quercetin (the chosen standard) in Table 2 could be the cause of this weak interaction.

The *in silico* screening of our derivative shows considerable pharmacological properties responsible for the reactive oxidative species scavenging attribute. However, the low docking affinity could be modified for a better functional group for improved affinity in the development of alternative therapy for abating oxidative stress.

Thermodynamic functions such as Gibbs free energy, enthalpy, dipole moment, and electronic energy are essential thermodynamic parameters for the description of ligand-receptor interactions. These parameters are computed to speculate on the spontaneity of a chemical reaction and the chemical stability of a reaction. As a parameter, enthalpy measures the total thermodynamic energy [40]. This means the compound requires no external energy to be reactive, as they both are more negative, with potentially reduced energy release during an exothermic reaction to break the interaction bond. The dipole moment clarifies the polarity, and the electron distribution dictates the compound property. This parameter enhances the binding affinity, non-bonded interactions, and hydrogen bond formation with the receptor protein [20,41].

Both the highest occupied molecular orbital (HOMO) and the lowest unoccupied molecular orbital (LUMO) are parameters used to understand the electron-accepting and -donating ability of a compound. While the HOMO signifies the electron denoted, the LUMO indicates the electron accepted, and they are crucial orbital measurements for the chemical stability of compounds [19,41]. For optimized KAD-3, the energy band gap (eV) is a function of the HOMO and LUMO difference and is used to determine the chemical reactivity and kinetic stability of a compound. A large band gap is a characteristic of a less reactive but more stable interaction, and vice versa. The values of the energy band gap are in order: quercetin < KAD-3. This indicates KAD-3 has a high kinetic stability but a reduced reactivity than quercetin.

The ionization energy (I) shows the energy required to adequately eliminate an electron from a molecule. A low ionization energy denotes better reactivity and lowered chemical inertness, and vice versa. KAD-3 has a higher ionization energy than the standard, which indicates a high degree of stability and chemical inertness. Also, electron affinity (A) represents the amount of energy liberated upon the addition of an electron to a neutral molecule [20]. A compound with high electron affinity accepts free electrons, making it reactive. Quercetin at 1.84 eV shows a better reactive tendency than KAD-3 at 1.42 eV. Chemical hardness and softness are two parameters that explain the stability and chemical reactivity of a molecule. As though, hard molecules possess a bigger energy band gap and vice versa for softness [41].

KAD-3 (2.20 eV) is harder than Quercetin (1.82 eV), and also calculated to have a characteristically lowered softness as represented in Table 2. This signifies quercetin as being easily polarizable. For the chemical potential, chemical species are able to accept surrounding electrons that are electrophiles through the charge transfer path. This resulted in a negative electronic chemical potential and a lower energy than the accepted electronic charge, which connote stable ligand-receptor complex formation [42]. The ability of this compound to attract electrons, termed electronegativity (χ) is more pronounced in quercetin than KAD-3. Overall, this compound had a significant level of reactivity compared to the standard.

5. Conclusions

As the need for more efficient, safe and natural compounds increases, there have been conscious studies on different class of phytochemicals with the aforementioned potential. Therefore, our study was with purpose in this direction for drug design and development to disease like diabetes mellitus and other related cardiovascular disease. The overall finding of the experimental and computational studies suggest that KAD-3 could be used to treat and manage oxidative hepatic damage in a variety of ways. The ability of KAD-3 to reduce oxidative stress and control nucleotide hydrolysis all points to the therapeutic and protective potential of KAD-3 against oxidative hepatic toxicity. Additionally, the molecular docking outcome display a need for advance optimization of the lead for better affinity than the standard quercetin. The ADME/Tox profile indicated the compound to be toxic free, and having preferred physiochemical and pharmacokinetic values of a potential drug. More so, the DFT analysis of the present study suggest that KAD-3 is in agreement to the possession of a good reactivity, kinetic stability, harness, softness and polarization of a good drug candidate. As a result, KAD-3 is suitable as precursor in drug formulation for diabetes management and treatment.

Ethical approval

Rats were kept in agreement with the approved policies of BUI Institutional Animal Ethics Committee, and the study was given their approval (approval number: BUI/BCH/2022/0002). The date of approval was 21st May 2022.

Author contributions

Conceptualization, OAO., ADO. and ABO.; methodology, MI., OAT., CBO., AA., DF., AIO., GAG., CON., ABO., ADO., OOO, and OAO.; investigation, AA., DF., OAT., CBO., MI., GAG., AIO., CON., ABO., ADO., OOO., and OAO.; data curation, AA., DF., OAT., CBO., MI., AIO., GAG., CON., ABO., ADO., OOO., and OAO.; writing—original draft preparation, OAT., CBO., MI., CON., ABO., ADO., OOO., and OAO.; writing—review and editing, CBO., MI., CON., ABO., OOO., and OAO. All authors have read and agreed to the published version of the manuscript.

Funding

This research received no external funding.

Informed consent statement

Not applicable.

Data availability statement

Data available on reasonable request.

Declaration of competing interest

The authors declare that they have no known competing financial interests or personal relationships that could have appeared to influence the work reported in this paper.

Acknowledgement

Author wish to acknowledge the Department of Biochemistry, Bowen University for providing the facilities to carry out the research.

References

[1] van Raamsdonk JM, Vega IE, Brundin P. Oxidative stress in neurodegenerative disease: causation or association? Oncotarget 2017;8:10777–8. https://doi.org/10.18632/oncotarget.14650.
[2] Ojo OA, Ojo AB, Okolie C, Nwakama MAC, Iyobhebhe M, Evbuomwan IO, Nwonuma CO, Maimako RF, Adegboyega AE, Taiwo OA, et al. Deciphering the interactions of bioactive compounds in selected traditional medicinal plants against alzheimer's diseases via pharmacophore modeling, auto-QSAR, and molecular docking approaches. Molecules 2021;26. https://doi.org/10.3390/molecules26071996.
[3] Ojo OA, Amanze JC, Oni AI, Grant S, Iyobhebhe M, Elebiyo TC, Rotimi D, Asogwa NT, Oyinloye BE, Ajiboye BO, et al. Antidiabetic activity of avocado seeds (persea americana mill.) in diabetic rats via activation of PI3K/AKT signaling pathway. Sci Rep 2022;12:1–18. https://doi.org/10.1038/s41598-022-07015-8.
[4] Thomford NE, Senthebane DA, Rowe A, Munro D, Seele P, Maroyi A, Dzobo K. Natural products for drug discovery in the 21st century: innovations for novel drug discovery. Int J Mol Sci 2018;19(6):1578.
[5] Tresserra-Rimbau A, Lamuela-Raventos RM, Moreno JJ. Polyphenols, food and pharma. Current knowledge and directions for future research. Biochem Pharmacol 2018;156:186–95.
[6] Kumar N, Goel N. Phenolic acids: natural versatile molecules with promising therapeutic applications. Biotechnology Reports 2019;24:e00370.
[7] Hanhineva K, Törrönen R, I.B P-I. Journal of, undefined impact of dietary polyphenols on carbohydrate metabolism. mdpi.com; 2010.
[8] Adisakwattana S. Cinnamic acid and its derivatives: mechanisms for prevention and management of diabetes and its complications. Nutrients 2017;9. https://doi.org/10.3390/nu9020163.
[9] De Cássia Da Silveira E Sá R, Andrade LN, Dos R, Barreto De Oliveira R, Pergentino De Sousa D. A review on anti-inflammatory activity of phenylpropanoids found in essential oils. mdpi.com 2014;19:1459–80. https://doi.org/10.3390/molecules19021459.
[10] Anantharaju PG, Gowda PC, Vimalambike MG, Madhunapantula SV. An overview on the role of dietary phenolics for the treatment of cancers. Nutr J 2016;15. https://doi.org/10.1186/S12937-016-0217-2.
[11] Küçükgüzel I, Küçükgüzel S. S.R.-B.& medicinal; undefined some 3-thioxo/Alkylthio-1, 2, 4-triazoles with a substituted thiourea moiety as possible Antimycobacterials. Elsevier; 2001.
[12] Ojo AB, Gyebi GA, Alabi O, Iyobhebhe M, Kayode AB, Nwonuma CO, Ojo OA. Syzygium aromaticum (L.) merr. & L.M.perry mitigates iron-mediated oxidative brain injury via in vitro, ex vivo, and in silico approaches. J Mol Struct 2022;1268:133675. https://doi.org/10.1016/J.MOLSTRUC.2022.133675.
[13] Salau VF, Erukainure OL, Islam M. Caffeic acid protects against iron-induced cardiotoxicity by suppressing angiotensin-converting enzyme activity and modulating lipid spectrum, gluconeogenesis and nucleotide hydrolyzing enzyme activities. Biol Trace Elem Res 2021;199:1052–61.
[14] Erukainure OL, Mopuri R, Oyebode OA, Koorbanally NA, Islam MS. Dacryodes edulis enhances antioxidant activities, suppresses DNA fragmentation in oxidative pancreatic and hepatic injuries; and inhibits carbohydrate digestive enzymes linked to type 2 diabetes. Biomed Pharmacother 2017;96:37–47.
[15] Kozakov D, Grove LE, Hall DR, Bohnuud T, Mottarella SE, Luo L, Xia B, Beglov D, Vajda S. FTMap family of web servers for determining and characterizing ligand-binding hot spots of proteins. Nat Protoc 2015;10(5):733–55.
[16] Schöning-Stierand K, Diedrich K, Fährrolfes R, Flachsenberg F, Meyder A, Nittinger E, Steinegger R, Rarey M. ProteinsPlus: interactive analysis of protein–ligand binding interfaces. Nucleic Acids Res 2020;48:W48–53.
[17] Omoboyede V, Ibrahim O, Umar HI, Bello T, Adedeji AA, Khalid A, Fayojegbe ES, Ayomide AB, Chukwuemeka PO. Designing a vaccine-based therapy against Epstein-Barr virus-associated tumors using immunoinformatics approach. Comput Biol Med 2022;150:106128.
[18] Olowosoke CB, Alaba AA, Adegboye BB. Citrullus lanatus natural product library: a hoard of viable potential inhibitor candidates for diabetes mellitus type II therapeutic target enzymes. World J Adv Res Rev 2020;15:534–60. https://doi.org/10.30574/wjarr.2022.15.1.0713. 01.
[19] Bashir L, Saidu S, Onikanni AS, Yunusa OI, Abdulhakeem RA, Halimat YL, Femi O, Ali AJ, Batiha G, Shukurat BB, Gomaa M, Clara MGL, Alexander THW, Hsu-Shan H, Carlos AC. Preclinical anti-inflammatory and antioxidant effects of Azanza garckeana in STZ-induced glycemic-impaired rats, and pharmacoinformatics of it major phytoconstituents. Biomed Pharmacother 2022;152(2022):113196.
[20] Olowosoke CB, Otitoola SG, Alaba AA, Adepoju OH, Okorie B, Odjegba PI, Ogunsanmi AO, Oke GA, Akinlolu O, Olubena TL, Bello RO, Adegboye BB. Insilico validation of selected natural products as multi-regulator of EZH2-PPAR therapeutic targets. A Hallmark for Prospective Restoration of Pancreatic Insulin Production and Cancer dysregulation 2022. https://doi.org/10.21203/rs.3.rs-2016513/v1. PREPRINT (Version 1) available at Research Square.
[21] Grimme S, Antony J, Ehrlich S, Krieg H. A consistent and accurate ab initio parametrization of density functional dispersion correction (DFT-D) for the 94 elements H-Pu. J Chem Phys 2010;132(15):154104.
[22] Das G, Shin HS, Patra JK. Comparative assessment of antioxidant, anti-diabetic and cytotoxic effects of three peel/shell food waste extract-mediated silver nanoparticles. Int J Nanomed 2020;15:9075–88. https://doi.org/10.2147/IJN.S277625.
[23] Liang C, Zhang X, Yang M, Dong X. Recent progress in ferroptosis inducers for cancer therapy. 2019. p. 1–25. https://doi.org/10.1002/adma.201904197. vol. 1904197.
[24] Shin SK, Cho HW, Song SE, Song DK. Catalase and nonalcoholic fatty liver disease. Pflügers Arch. - Eur. J. Physiol. 2018;470:1721–37. https://doi.org/10.1007/S00424-018-2195-Z. 47012 2018.
[25] Ho Y, Xiong Y, Ma W, Spector A. Chemistry, D.H.-J. Of B.; undefined mice lacking catalase develop normally but show differential sensitivity to oxidant tissue injury. ASBMB; 2004.
[26] Ajiboye BO, Oyinloye BE, Agboinghale PE, Ojo OA. Cnidoscolus aconitifolius (mill.) I. M. Johnst leaf extract prevents oxidative hepatic injury and improves muscle glucose uptake ex vivo. J Food Biochem 2019;43. https://doi.org/10.1111/jfbc.13065.
[27] Ojo OA, Oni AI, Grant S, Amanze J, Ojo AB, Taiwo OA, Maimako RF, Evbuomwan IO, Iyobhebhe M, Nwonuma CO, et al. Antidiabetic activity of elephant grass (cenchrus purpureus (schumach.) morrone) via activation of PI3K/AkT signaling pathway, oxidative stress inhibition, and apoptosis in wistar rats. Front Pharmacol 2022;13:1–15. https://doi.org/10.3389/fphar.2022.845196.
[28] Ojo OA, Ojo AB, Nwonuma CO, Josephine O, Maimako RF, Taiwo OA, et al. A review on the pharmacological activity, chemical properties and pharmacokinetics of main isoflavonoid. Nat Prod J 2022;12(1). https://doi.org/10.2174/2210315510999201105145149. e160921187628.
[29] Alevizopoulos K, Calogeropoulou T, Lang F, Stournaras C. Na+/K+ ATPase inhibitors in cancer. Curr Drug Targets 2014;15(10):988–1000.
[30] Srikanthan K, Shapiro JI, Sodhi K. The role of Na/K-ATPase signaling in oxidative stress related to obesity and cardiovascular disease. Molecules 2016 Sep;21(9):1172.
[31] Liu J, Lilly MN, Shapiro JI. Targeting Na/K-ATPase signaling: a new approach to control oxidative stress. Curr Pharmaceut Des 2018;24(3):359–64.
[32] Liu J, Chaudhry M, Bai F, Chuang J, Chaudhry H, Al-Astal AE, Nie Y, Sollars V, Sodhi K, Seligman P, Shapiro JI. Blockage of the Na-K-ATPase signaling-mediated oxidant amplification loop elongates red blood cell half-life and ameliorates uremic anemia induced by 5/6th PNx in C57BL/6 mice. Am. J. Physiol. Ren. Physiol. 2022;322(6):F655–66.
[33] Zhou Y, Zhang H, Chen D, Chen Z, Li Y, Tian C, Zhang C, Li C, Chang B, Zeng R, Li J. A small-molecule lycorine derivative reveals Na+/K+-ATPase α3 as an anti-obesity target. bioRxiv preprint 2022;2022. https://doi.org/10.1101/2022.08.24.505199.
[34] Ajiboye BO, Ojo OA, Okesola MA, Oyinloye BE, Kappo AP. Ethyl acetate leaf fraction of cnidoscolus aconitifolius (mill.) I. M. Johnst: antioxidant potential, inhibitory activities of key enzymes on carbohydrate metabolism, cholinergic, monoaminergic, purinergic, and chemical fingerprinting. Int J Food Prop 2018;21:1697–715. https://doi.org/10.1080/10942912.2018.1504787.
[35] Gorelik A, Labriola JM, Illes K, Nagar B. Crystal structure of the nucleotide-metabolizing enzyme NTPDase4. Protein Sci 2022;29(10):2054–61.
[36] Zhang N, Wang J-X, Wu X-Y, Cui Y, Zou Z-H, Liu Y, Gao J. Correlation analysis of plasma myeloperoxidase level with global registry of acute coronary events score and prognosis in patients with acute non-ST-segment elevation myocardial infarction. Front Med 2022;9:828174.
[37] Al-Rashida M, Iqbal J. Therapeutic potentials of ecto-nucleoside triphosphate diphosphohydrolase, ecto-nucleotide pyrophosphatase/phosphodiesterase, ecto-5'-nucleotidase, and alkaline phosphatase inhibitors. Med Res Rev 2014;34(4):703–43. https://doi.org/10.1002/med.21302. 2014.
[38] Udoikono AD, Louis H, Eno EA, Agwamba EC, Unimuke TO, Igbalagh AT, Edet HO, Odey JO, Adeyinka AS. Reactive azo compounds as a potential chemotherapy drugs in the treatment of malignant glioblastoma (GBM): experimental and theoretical studies. J Photochem Photobiol, A 2022;10:100116.
[39] Ojo OA, Ojo AB, Okolie C, Abdurrahman J, Barnabas M, Evbuomwan IO, Atunwa OP, Atunwa B, Iyobhebhe M, Elebiyo TC, et al. Elucidating the interactions of compounds identified from aframomum melegueta seeds as promising candidates for the management of diabetes mellitus: a computational approach. Inform Med Unlocked 2021;26:100720. https://doi.org/10.1016/j.imu.2021.100720.

[40] Garbett NC, Chaires JB. Thermodynamic studies for drug design and screening. Expet Opin Drug Discov 2012;7(4):299–314. https://doi.org/10.1517/17460441.2012.666235.

[41] Balogun TA, Ipinloju N, Abdullateef OT, Moses SI, Omoboyowa DA, James AC, Saibu OA, Akinyemi WF, Oni EA. Computational evaluation of bioactive compounds from colocasia affinis schott as a novel EGFR inhibitor for cancer treatment. Cancer Inf 2021;20:11769351211049244. 10.1177%2F11769351211049244.

[42] Iwaloye O, Elekofehinti OO, Olawale F, Chukwuemeka PO, Babatomiwa K, Foloruso IM. Fragment-based drug design, 2D-QSAR and DFT calculation: scaffolds of 1, 2, 4, triazolo [1, 5-a] pyrimidin-7-amines as potential inhibitors of *plasmodium falciparum* dihydroorotate dehydrogenase. Lett Drug Des Discov 2022;19. 000-000.